JACS
JOURNAL OF THE AMERICAN CHEMICAL SOCIETY

Article

pubs.acs.org/JACS

"Minimalist" Cyclopropene-Containing Photo-Cross-Linkers Suitable for Live-Cell Imaging and Affinity-Based Protein Labeling

Zhengqiu Li, Danyang Wang, Lin Li, Sijun Pan, Zhenkun Na, Chelsea Y. J. Tan, and Shao Q. Yao*

Department of Chemistry, National University of Singapore, 3 Science Drive 3, Singapore 117543

Supporting Information

ABSTRACT: Target identification of bioactive compounds within the native cellular environment is important in biomedical research and drug discovery, but it has traditionally been carried out in vitro. Information about how such molecules interact with their endogenous targets (on and off) is currently highly limited. An ideal strategy would be one that recapitulates protein−small molecule interactions in situ (e.g., in living cells) and at the same time enables enrichment of these complexes for subsequent proteome-wide target identification. Similarly, small molecule-based imaging approaches are becoming increasingly available for in situ monitoring of a variety of proteins including enzymes. Chemical proteomic strategies for simultaneous bioimaging and target identification of noncovalent bioactive compounds in live mammalian cells, however, are currently not available. This is due to a lack of photoaffinity labels that are minimally modified from their parental compounds, yet chemically tractable using copper-free bioorthogonal chemistry. We have herein developed novel minimalist linkers containing both an alkyl diazirine and a cyclopropene. We have shown chemical probes (e.g., **BD-2**) made from such linkers could be used for simultaneous in situ imaging and covalent labeling of endogenous BRD-4 (an important epigenetic protein) via a rapid, copper-free, tetrazine-cyclopropene ligation reaction ($k_2 > 5\ M^{-1}\ s^{-1}$). The key features of our cyclopropenes, with their unique C-1 linkage to BRD-4-targeting moiety, are their tunable reactivity and solubility, relative stability, and synthetic accessibility. **BD-2**, which is a linker-modified analogue of (+)-JQ1 (a recently discovered nanomolar protein−protein-interaction inhibitor of BRD-4), was subsequently used in a cell-based proteome profiling experiment for large-scale identification of potential off-targets of (+)-JQ1. Several newly identified targets were subsequently confirmed by preliminary validation experiments.

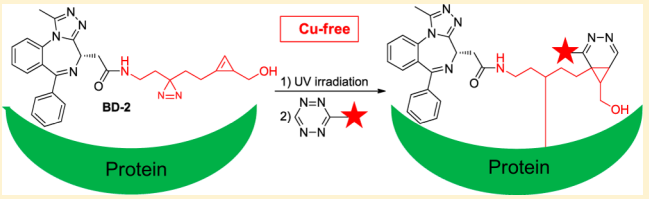

INTRODUCTION

Target identification of small molecule-based bioactive compounds within the native cellular environment is important in biomedical research and drug discovery, but has traditionally been carried out in vitro by using recombinant proteins or crude cellular lysates.[1] Information about how such molecules interact with their endogenous targets (on and off) is therefore highly limited.[2] An ideal strategy would be one that recapitulates protein−small molecule interactions in situ (e.g., in living cells), and at the same time enables enrichment of these complexes for subsequent proteome-wide target identification.[3] In the past several years, by taking cue from concepts developed for activity-based protein profiling,[4] cell-based proteome profiling methods have emerged; drug-like chemical probes minimally modified from their parental compounds have been used for large-scale interrogation of protein−small molecule interactions and rapid identification of potential cellular targets in live cells.[3,5,6] Such an "in situ drug-profiling" approach is applicable to compounds that form either irreversible or reversible complexes with their intended targets.[7−9] The probe design involves introduction of a chemically "tractable" handle, which should not disrupt protein−ligand interaction in situ. So far, the handle-of-choice has been a terminal alkyne because it is small, chemically inert and can be further modified for downstream proteomic applications with azide-containing reporters via copper-catalyzed alkyne−azide cycloaddition (CuAAC).[10] In the case of noncovalent bioactive compounds, which account for >95% of all FDA-approved drugs and candidates, another key consideration is the introduction of an additional photoreactive moiety within the probe for on-demand (e.g., by UV irradiation), in-cell conversion of transient protein−ligand complexes into stable, covalent ones (Figure 1A).[8,9] Such photoaffinity labeling (PAL) approaches had previously been used to study different types of noncovalent interactions.[11] In the context of "drug profiling", however, the key requirement is the chemically tractable photo-cross-linker must be made as small as possible.[3] Our recently developed first-generation "minimalist" linkers, which contain an alkyl diazirine and a terminal alkyne connected by short aliphatic chains, fulfill such a requirement, and have been used to tag many kinase inhibitors with minimal loss in their native biological activities (Figure 1A).[9] But they fall short of being ideal due to the need of Cu(I) catalysts in CuAAC, and thus are ineffective in events where both photo-cross-linking and reporter-tagging (e.g., in

Received: March 19, 2014
Published: June 27, 2014

   dx.doi.org/10.1021/ja502780z | J. Am. Chem. Soc. 2014, 136, 9990−9998

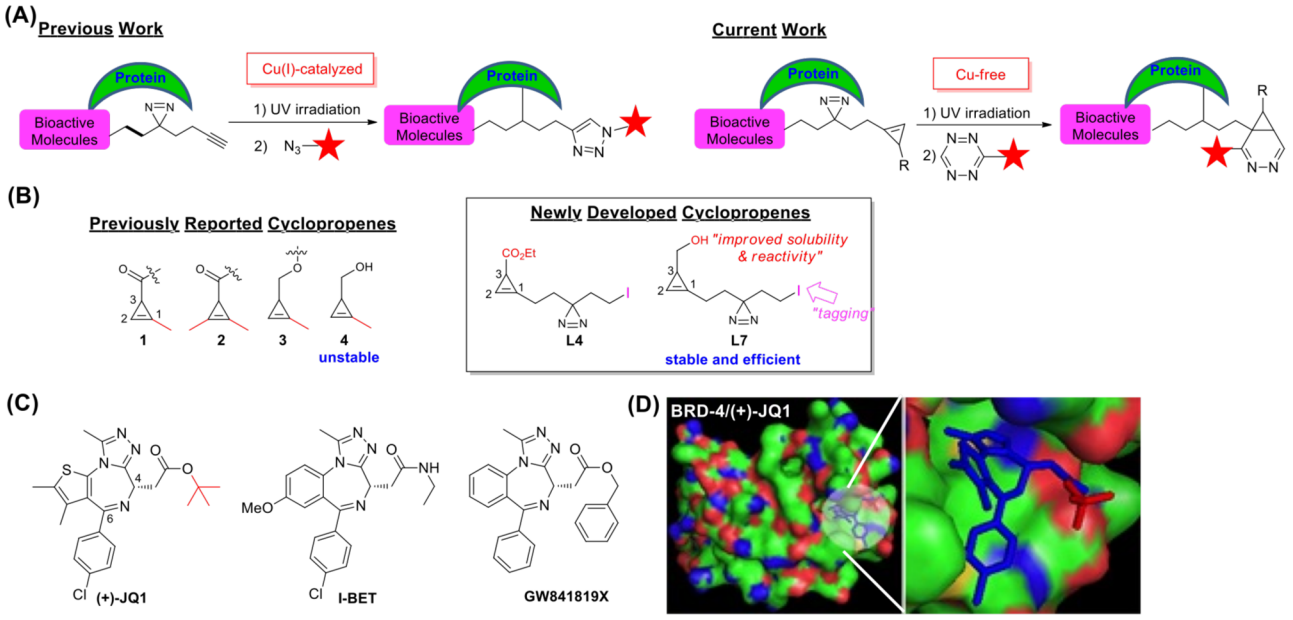

Figure 1. (A) Two drug-profiling PAL approaches: (left) previously developed approach in which bioactive compounds were "tagged" with first-generation "minimalist" linkers;[9] (right) second-generation approach reported in the current work, with cyclopropenes as chemically tractable tags suitable for copper-free bioorthogonal chemistry. (B) Structures of previously reported cyclopropenes (**1**−**4**),[18−20] and newly reported ones (**L4** and **L7**; boxed). (C) Known BRD-4-targeting compounds. (D) the X-ray complex (PDB code: 3MXF) of BRD-4/(+)-JQ1 showing the active-site binding (right panel).[24a]

bioimaging applications[12]) are conducted simultaneously in situ. Weissleder et al. recently reported *trans*-cyclooctene (TCO)-modified kinase inhibitors with tetrazine-containing fluorescent reporters for live-cell imaging of kinase activities.[12a,b] Other small molecule-based imaging approaches have also become increasingly available for in situ monitoring of a variety of proteins including enzymes.[12c−h] While elegantly designed and effective, Weissleder's kinase-imaging probes have some room for further improvement. For example, the replacement of the relatively bulky TCO moiety with smaller "clickable" tags and the introduction of a photo-cross-linker would render this strategy suitable for above-mentioned in situ imaging/profiling applications.[13] We previously showed that chemical modifications of bioactive compounds with "tags" of different sizes had a significant effect on target recognition.[8] Furthermore, introduction of a covalent linkage between a potentially diffusible small molecule imaging probe and its intended targets has been shown to further improve imaging resolution in situ by effectively "fixing" the probe near the reaction site.[14] Herein, we report the development of **L4** and **L7**, our second-generation minimalist linkers (Figure 1B; boxed), which contain a novel cyclopropene handle and a diazirine within the same molecule, and their successful incorporation into protein−protein-interaction (PPI) inhibitors of BET bromodomains (e.g., BRD-4; Figure 1C,D). We show, for the first time, chemical probes made from such linkers could be used for simultaneous imaging and protein labeling in live cells via copper-free tetrazine-cyclopropene ligation reaction.

RESULTS AND DISCUSSION

Design and Synthesis. In order to render our first-generation minimalist linkers copper-free, we surveyed numerous "handles" used in bioorthogonal chemistry as possible replacement of terminal alkynes.[15−17] An $-N_3$ handle was initially considered as it is small and has been widely used for metabolic incorporation of unnatural amino acids, carbohydrates and lipids.[15] We were however worried about its susceptibility to be reduced by endogenous thiols. Strained alkenes/alkynes (i.e., TCO, norborenes, cyclooctynes) as well as tetrazines are also amenable to metabolic incorporation, but most of them are too bulky for our applications.[16,17] We chose substituted cyclopropenes, which are similar in size to a terminal alkyne, metabolically stable, and undergo rapid bioorthogonal reaction with a suitable tetrazine (e.g., a second-order rate constant k_2 of up to 13 M^{-1} s^{-1} for **3**).[18] We were also intrigued by the tunability of both the stability and reactivity in cyclopropenes, which are affected sterically and electronically by their C-1/C-2/C-3 substituents (Figure 1B, **1**−**4**).[18,19] These features might be further explored in multiplex experiments by using mutually exclusive cyclopropene pairs.[20] The relative chemical instability of both alkyl diazirines and cyclopropenes was another concern in our linker design. As unhindered cyclopropenes are prone to self-polymerization and attack by biological nucleophiles,[18,19] and both cyclopropenes and diazirines are sensitive to harsh reaction conditions, having them present within the same linker poses significant synthetic challenges. Finally, we settled on the two diazirine-containing cyclopropene linkers, **L4**/**L7**. Unlike other reported cyclopropenes, where compounds were linked at C-3 position,[18−21] we chose to attach compounds via C-1 linkage (Figure 1B). This offers several advantages: (1) C-3 is now available for further tuning of the cyclopropene's reactivity and solubility; (2) C-1 attachment offers the needed steric hindrance in the resulting cyclopropenes for improved stability without introducing an additional methyl at either C-1 or C-2 position (e.g., **1**-**4** in Figure 1B); (3) **L4**/**L7** are now synthetically accessible from their terminal-alkyne precursors (e.g., our first-generation linkers[9]) by using the well-established rhodium-catalyzed reaction of α-diazo esters with alkynes.[22]

Synthesis of **L4** was accomplished from the previously reported **L3** by treatment with commercially available ethyl

dx.doi.org/10.1021/ja502780z | J. Am. Chem. Soc. 2014, 136, 9990−9998

diazoacetate and a catalytic amount of $Rh_2(OAc)_4$ (Scheme 1).[9] The single-step synthesis of **L4** from **L3** clearly outweighs its

Scheme 1. Synthesis of Diazirine Containing Cyclopropene Linkers (L4/L7) and BRD-4 Targeting Probes (BD-1/3)

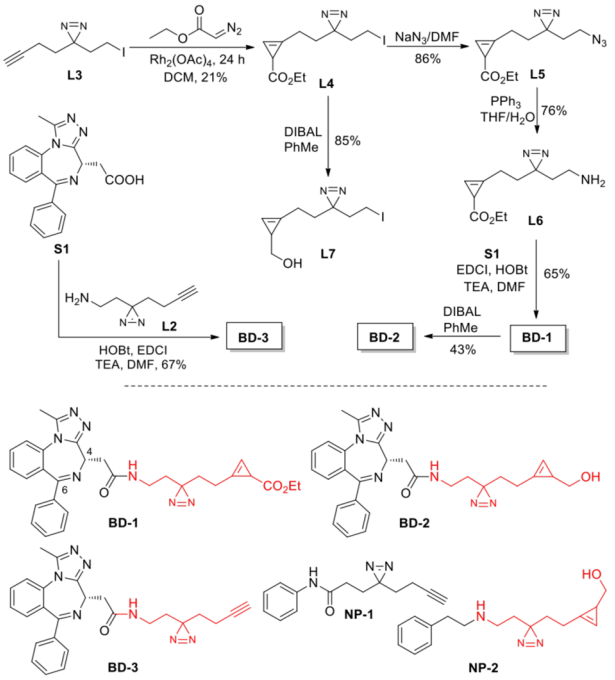

relatively low yield (21%). Further DIBAL reduction of the C-3 ester in **L4** afforded **L7** in excellent yield (85%). It should be noted that, unlike reported cyclopropenes (**1**−**4**),[18−20] which needed obligatory TMS protection at either C-1 or C-2 position during synthesis, both **L4** and **L7** were stable under our reaction conditions without any special handling. With these second-generation minimalist linkers, we next used them to make BRD-4 targeting chemical probes (**BD-1** and **BD-2**). BRD-4 is a BET bromodomain that recognizes acetylated lysine (Kac) residues such as those located on histones. It is an important epigenetic "reader" involved in chromatin remodeling, DNA damage, cell-cycle control and other critical cellular processes.[23] Recent findings that benzodiazepine-containing compounds such as (+)-JQ1, I-BET and GW841819X (Figure 1C) are nanomolar PPI inhibitors of BRD-4 have spurred enormous interests to further develop such compounds into potential drugs against diseases including cancer, HIV infection and heart disease.[24,25] Previous proteomic study was carried out, in an in vitro pull-down experiment by using an immobilized I-BET analogue together with mammalian cell lysates, to unequivocally identify BRD-4 as the endogenous target of these compounds.[26] Their potential off-targets, however, have not been investigated at the proteome level in situ (e.g., in live cells, not lysates), due to a lack of suitable chemical probes. On the basis of the published X-ray structure of (+)-JQ1/BRD-4 complex (Figure 1D),[24a] substituents at C_6 and on both the triazole and thiophene rings in (+)-JQ1 were critical in binding to the Kac-binding pocket of BRD-4, while the *t*-butylacetyl group at C_4 was nonessential. A recent study showed surface-immobilized (+)-JQ1 via C_4 linkage retained its full BRD-4 binding property.[27] We thus expected that, with an C_4 appendage to **L4**/**L7**, both **BD-1** and **BD-2** should maintain similar protein-binding property as their parental compound GW841819X (a close analogue of (+)-JQ1).[26] To synthesize **BD-1**/**2**, **L4** was first converted to **L5** with NaN_3 (86% yield), then reduced to **L6** with PPh_3/H_2O/THF (76%). Subsequent coupling between **L6** and **S1** afforded **BD-1** (65%), which was further reduced to give **BD-2** (43%). **BD-3** (a reference probe tagged with our first-generation minimalist linker) and **NP-1**/**NP-2** (negative control probes for **BD-3**/**BD-2**, respectively) were similarly synthesized. With an electron-donating hydroxymethyl group at C-3 position in the cyclopropene of **BD-2**, we expected this probe, compared to **BD-1**, to possess better water solubility and faster ligation toward tetrazine-containing reporters.

Ligation Studies with Different Tetrazines. With these probes in hand, we first examined the tetrazine-ligation reactivity and biocompatibility of **L4**/**L7** (Figure 2). Cyclopropene **5** was tested concurrently as a reference compound.[18] Different tetrazines (**6**−**8**; Figure 2C), including **Biotin-TZ2** (**8**), were used, and the ligation reactions were monitored by both LC−MS (Figures S1−S7, Supporting Information), and spectrometric measurement of disappearance in the tetrazine absorption band at 520 nm to obtain the second-order rate constant (Figure 2B−D; Figures S10 and S11, Supporting Information). We obtained a rate constant of 5.03 ± 0.34 M^{-1} s^{-1} for **L7** with **8**, which is similar to one of the fastest tetrazine-cyclopropene ligations reported (e.g., k_2 up to 13 M^{-1} s^{-1} with cyclopropene **3**[18]). As expected, **L4**, with an electron-withdrawing C-3 ester, reacted sluggishly (k_2 = 0.31 × 10^{-2} M^{-1} s^{-1} with **8**), comparable to that of **5** under identical assay conditions (k_2 = 0.56 × 10^{-2} M^{-1} s^{-1}). Similar reactivity trends between **L4** and **L7** with other tetrazines were observed (Figure 2C); in all cases, **L7** consistently reacted between 10- to 2000-fold faster than **L4**, with k_2 ranging from 0.1 to 5.03 M^{-1} s^{-1}. While these reactions are slower than some other tetrazine-based ligations,[16,17] they are still much faster than the Staudinger ligation (k_2 < 0.01 M^{-1} s^{-1}), a bioorthogonal reaction widely used in live cells and animals.[15] A representative ligation reaction is shown in Figure 2A, with the structure of the expected ligation products confirmed by both LC−MS and NMR (Figure S1, Supporting Information). Although asymmetric cyclopropene/tetrazine ligation could produce up to 4 different diastereomers,[18−20] we were unable to chromatographically separate them. Ligation products from cyclopropenes that contain a suitable C-3 nucleophile were previously shown to undergo further intramolecular cyclization (Figure S2, Supporting Information);[19] no such evidence was found in our system.

Biocompatibility and Turn-ON Properties of L7. The cyclopropene moiety in **L7** was found to be highly stable in aqueous buffers and in the presence of biological nucleophiles (L-cysteine) for extended periods of time (Figures S8 and S9, Supporting Information), thus making them suitable for in situ applications. Weissleder et al. recently showed tetrazines could effectively quench the fluorescence of several organic fluorophores, and the authors further exploited this unique feature in live-cell bioimaging to minimize nonspecific background fluorescence labeling, by making use of tetrazine-containing fluorogenic reporters whose fluorescence was "Turned-ON" only upon ligation with a strained dienophile.[12a,b] We wondered whether such a system might work with our newly developed diazirine-containing cyclopropenes. As shown in Figure 2D,E, with a cell-permeable, tetrazine-containing fluorogenic reporter **FL-TZ1**, the intrinsic fluorescence of its deacetylated form, **S10**, went from the "OFF" to

dx.doi.org/10.1021/ja502780z | J. Am. Chem. Soc. 2014, 136, 9990−9998

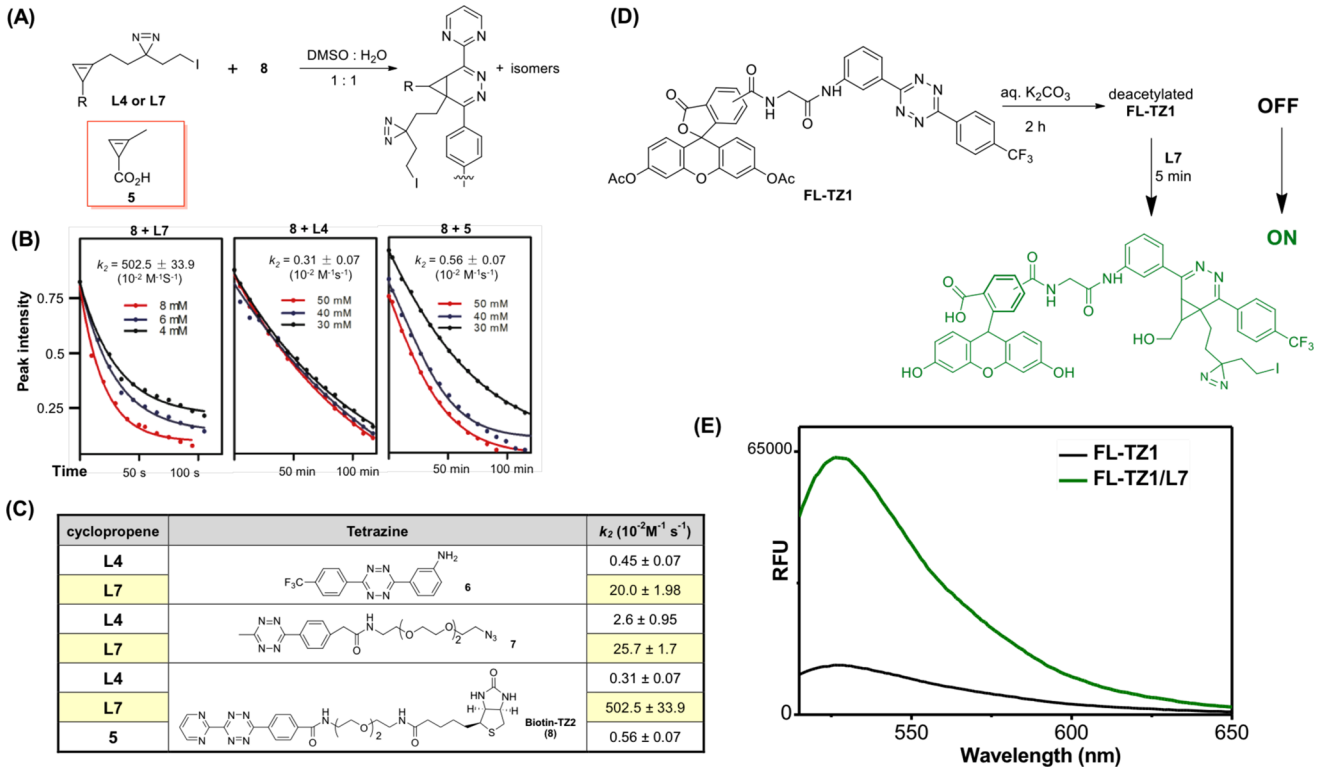

Figure 2. (A) Scheme of tetrazine **8** reacting with cyclopropene **L4**, **L7** or **5**. Different diazanorcaradiene regioisomeric products could form, but for simplicity, only one regioisomer is depicted. (B) Plots of tetrazine absorbance (520 nm) versus time between ligation of **8** and **L7**, **L4** or **5**. Data was fitted to a first-order exponential decay to obtain the corresponding second-order rate constant (k_2). (C) k_2 of different tetrazines **6**, **7** or **8** reacting with **L7**, **L4** or **5**. (D) Schematic showing of ligation reaction between **FL-TZ1** and **L7**. (E) Emission spectra of deacetylated **FL-TZ1** alone, and 5 min after ligation with **L7**. 10 μL of **FL-TZ1** (10 mM in DMSO) was first treated with 20 μL of K_2CO_3 solution (100 mM) for 2 h at room temperature. Next, 40 μL of **L7** (15 mM in 10% DMSO/H_2O) was added, and the reaction mixture was incubated for 5 min. Upon dilution (500× with 10% DMSO/H_2O), the emission fluorescence was measured (λ_{ex} = 488 nm). Control sample was processed under the same conditions without addition of **L7**.

the fully "ON" state within 5 min of ligation with **L7**. The same effect was observed with a tetraethylrhodamine-containing reporter (Figure S10, Supporting Information).

Bioimaging and Affinity-Based Protein Labeling. We next assessed whether the two newly developed, cyclopropene-containing chemical probes could be used for simultaneous imaging and covalent labeling of BRD-4 protein. We first confirmed, in an isothermal titration calorimetry (ITC) experiment, that the probes could still bind to recombinant $(His)_6$-tagged BRD-4 protein with similar affinity as (+)-JQ1 (Figure 3A); the K_d values of **BD-2** (860 nM) and **BD-3** (810 nM) were both within ~2-fold range of that of (+)-JQ1 (390 nM) under identical assay conditions, thus confirming the minimal effect caused by C_4 modifications in (+)-JQ1 as previously reported.[24−27] We next showed both probes were able to efficiently label recombinant BRD-4 protein under UV-irradiation conditions (Figure 3B,C). First we carried out labeling with recombinantly purified BRD-4. Briefly, upon UV irradiation, the cross-linked protein/**BD-2** and protein/**BD-1** complexes were treated with **TER-TZ1** for different lengths of ligation time (1−60 min). For comparison, protein/**BD-3** complexes were "clicked" with **TER-N$_3$** under standard CuAAC conditions.[9] Labeled samples were separated and visualized by in-gel fluorescence scanning (Figure 3B); we observed strong fluorescent bands of **BD-2**/protein labeling in as little as 1 min of tetrazine-cyclopropene ligation reaction (right), with 1−20 μM of the probe (left). On the contrary, **BD-3**/protein labeling was detected only after 5−60 min of click reaction under CuAAC conditions. This highlights the extremely fast ligation reaction between the cyclopropene in **BD-2** and the tetrazine reporter. In comparison, fluorescent bands of **BD-1**/protein labeling reactions started to appear after 1 min of ligation (with **TER-TZ1**), but only reached a comparable level after 60 min. This agrees well with the ligation rate difference of **L4** and **L7** as earlier observed (Figure 2B,C). As **BD-2** appeared to be a more superior probe than **BD-1** in both its labeling efficiency and ligation speed, it was chosen for all subsequent studies. We next confirmed **BD-2** could be used to selectively label BRD-4 in a more complex environments (Figure 3C); a fluorescent band corresponding to the molecular weight of $(His)_6$-tagged BRD-4 was visible only in bacterial lysates overexpressing this protein, and the fluorescence intensity was abolished in the presence of excessive (+)-JQ1. Similar results were obtained with **BD-3**, the terminal alkyne-containing reference probe. Subsequently, in order to evaluate the live-cell imaging capability of **BD-2** toward BRD-4 endogenously expressed in mammalian cells, we directly added the probe to the medium of growing HepG2 cells, with or without 10 times of (+)-JQ1 as a competitor. Control experiments were carried out with **NP-2**. Upon UV irradiation to cross-link endogenous probe/protein complexes, the cells were directly treated with the cell-permeable **FL-TZ1**, then imaged (Figure 3D); strong green fluorescence signals were detected throughout the nucleus of labeled cells, which colocalized well with signals obtained from the immunofluorescence (IF) results with *anti*-BRD-4 antibody (see panel iv). No fluorescence was detected in cells treated

dx.doi.org/10.1021/ja502780z | J. Am. Chem. Soc. 2014, 136, 9990−9998

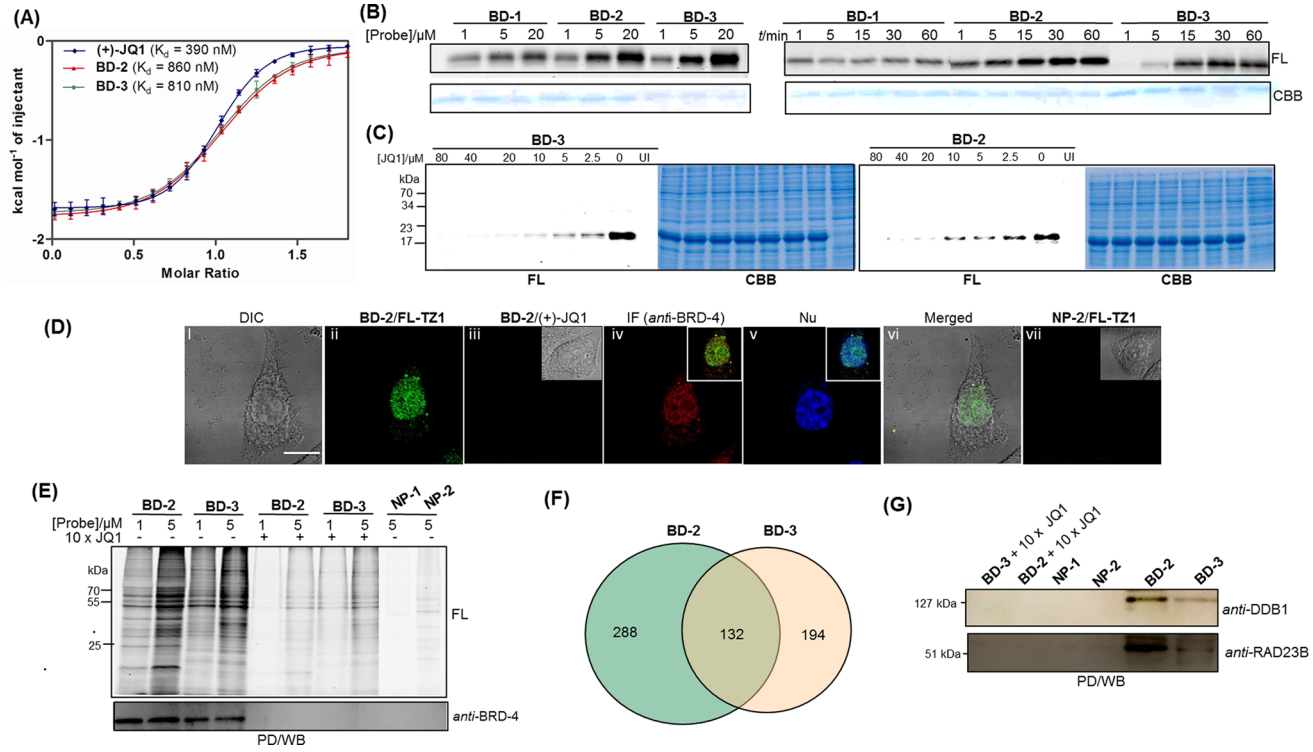

Figure 3. (A) ITC results of (+)-JQ1/**BD-2**/**BD-3** binding to $(His)_6$-tagged BRD-4. See Figure S12 (Supporting Information) for details. (B) Concentration-dependent labeling of **BD-1**/**2**/**3** with recombinant BRD-4 (2 μg; left gels), and time-dependent ligation (1−60 min; 5 μM probe) of probe-labeled BRD-4 with **TER-TZ1** (for **BD-1**/**2**) and **TER-N$_3$** (for **BD-3**). FL = in-gel fluorescence scanning. CBB = Coomassie gel. (C) Labeling of $(His)_6$-tagged BRD-4 overexpressing bacterial lysates by 1 μM of **BD-3** (left gels) or **BD-2** (right gels), in the presence of different amounts of (+)-JQ1 (0−80 μM), with **TER-TZ1** (10 μM; 2 h ligation). (D) Live-cell imaging of **BD-2**/**NP-2** (5 μM) followed by ligation with **FL-TZ1**. IF = immunofluorescence. Merged: panels i + ii. Insets in panels iv and v: merged panels ii/iv (with a Pearson's coefficient R = 0.76) and ii/v, respectively. Scale bar =10 μm. (E) In-gel fluorescence scanning showing the proteome reactivity profiles of live HepG2 cells labeled by **BD-2**/**BD-3**, with or without 10(+)-JQ1. The corresponding pull-down (PD)/Western blotting (WB) results are shown (bottom gel). For **BD-2**-labeled cells, ligation was done with **TER-TZ1**/**Biotin-TZ2**. **NP-1**/**NP-2**: negative control PD. (F) Venn diagram showing the number of proteins labeled/enriched by **BD-2**/**3** (1 μM) upon in situ labeling/PD/LC−MS/MS with live HepG2 cells. Nonspecific protein labeling was minimized by control labeling experiments with **NP** probes, and with 10(+)-JQ1. (G) Preliminary validation of the two newly identified off-targets of (+)-JQ1 by PD/WB from **BD-2** (1 μM)-labeled HepG2 cells. **BD-3** labeling was carried out concurrently as a reference. The corresponding control experiments were done with negative probes (**NP-1** and **NP-2**) and with 10(+)-JQ1.

with **NP-2** (panel vii), or with 10× competitive (+)-JQ1 (panel iii).

In Situ Target Identification and Validation. Next, the proteome reactivity profiles of the same in situ-labeled HepG2 cells were further analyzed (Figure 3E); upon cell lysis, the labeled samples were ligated with **TER-TZ1** (**TER-N$_3$** for **BD-3**-labeled samples), separated by SDS-PAGE, then analyzed by in-gel fluorescence scanning (top gel). Concurrently, a portion of the same sample was ligated with **Biotin-TZ2**, affinity-enriched on avidin-agarose beads, then separated, followed by Western blotting (WB) (bottom gel). A 73-kDa band in the pull-down (PD) samples treated with **BD-2** (1 and 5 μM) was successfully detected by *anti*-BRD-4 antibody, but not in samples labeled with **NP-2** or in the presence of 10× competitive (+)-JQ1, clearly showing the successful labeling of endogenous BRD-4 by **BD-2**. Similar in situ proteome labeling results were obtained with the reference probe **BD-3**. Interestingly, the proteome reactivity profiles of HepG2 cells labeled by **BD-2** and **BD-3**, though largely similar as one might expect, did show some minor but distinct differences (compare lanes 2 and 4 in Figure 3E top gel). This indicates the possible presence of both common and unique cellular targets of each probe (vide infra). We nevertheless could conclude that the newly developed cyclopropene-containing probe performed similarly as our first-generation, terminal alkyne-containing minimalist probe in cell-based proteome profiling experiments.

Finally, large-scale PD/LC−MS/MS analysis was carried out to delineate other unknown cellular targets (on and off) of (+)-JQ1, as well as to compare the difference in the performance between **BD-2** and **BD-3** (Figure 3F,G, Table 1,

Table 1. Selected High-Confidence Nuclear Proteins Enriched by Both BD-2 and BD-3

protein	mass (in Da)	protein score[a]	emPAI[a]
MYOF	236100	2195	0.75
DDB1	**128142**	**295**	**0.19**
USP7	117951	396	0.24
TXNRD1	60725	1993	3.15
HNRNPK	51230	1168	0.98
NAP1L1	44972	706	1.03
RAD23B	**43202**	**224**	**0.25**
CAPG	38760	282	0.28
PP2CA	36142	460	0.55

[a]Protein scores and emPAI values from **BD-2** samples are shown. For values from **BD-3** sample, see Table S3 (Supporting Information). Bolded proteins were further validated (Figure 3G).

dx.doi.org/10.1021/ja502780z | J. Am. Chem. Soc. 2014, 136, 9990−9998

and Supporting Information). In order to minimize "false hits" caused by non-specific protein binding and intrinsic non-specific labeling of PAL, proteins that appeared in LC−MS/MS results of experiments performed with negative probes (**NP-1** and **NP-2**) and with 10× (+)-JQ1 were removed. In addition, only proteins that appeared in duplicated/triplicated samples were considered further. At the end, we identified 420 and 326 candidates for **BD-2** and **BD-3**, respectively, in which ∼41% of the proteins (132; relative to 326) were pulled down by both probes (Figure 3F). Further analysis of these 132 proteins indicated a large number of them (49) were nuclear proteins (Table S3, Supporting Information). By analysis of putative (+)-JQ1 targets under more stringent criteria, we obtained 161 and 117 higher-confidence candidate proteins for **BD-2** and **BD-3**, respectively, with 48 overlapping proteins in which 14 were nuclear localized (Table S2, Supporting Information). Selected proteins are summarized in Table 1. It is somewhat surprising that, given the high degree of structural homology in **BD-2** and **BD-3**, only 41% of high-confidence proteins pulled-down by both probes were identical. This could be due to a number of factors: (1) the intrinsic variability of the instrument used in LC−MS/MS experiments. In fact, even with identical PD samples, duplicated/triplicated injections could only achieve, on average, 75% coverage of the same proteins; (2) the linker difference in **BD-2**/**BD-3**. Despite careful choices of linker appendage point and minimized linker size, the two probes afforded insignificant but noticeable differences in their proteome reactivity profiles as shown in Figure 3E. Future studies will need to be carried out to better understand the exact effect of linker on the outcome of off-target identification. Notwithstanding, with the dual capability of our new minimalist probes for both live-cell imaging and in situ proteome profiling, and the availability of different reporter tags (i.e., terminal alkyne and cyclopropene), these features were used to further improve the confidence level of candidate hits identified form our PD/LC−MS/MS experiments. Table 1 represents a list of selected proteins which are likely genuine off-targets of (+)-JQ-1, as they were both nuclear-localized (as supported by our imaging results) and successfully enriched by both **BD-2** and **BD-3**. We reasoned that a true cellular target of (+)-JQ1 would bind to both probes with similar affinity. In future proteomic experiments, such a combination approach by using both alkyne- and cyclopropene-tagged bioactive compounds might prove to be highly effective to help in the elimination of many potential false positives. To further confirm some of these proteins were indeed true cellular targets of (+)-JQ1, we carried out preliminary target validation experiments on two candidate proteins, DDB1 and RAD23B (Figure 3G). These two proteins were chosen because they are key proteins involved in DNA damage/repair pathways, and BRD-4 was recently found to be activated in response to DNA damage.[25b] By performing the same in situ proteome labeling/PD with live HepG2 cells and WB analysis of the enriched lysates with *anti*-DDB1 and *anti*-RAD23B antibodies, both proteins were successfully identified from both **BD-2** and **BD-3** labeled cells, but not with 10× (+)-JQ1, indicating they are likely true cellular targets of (+)-JQ1. We caution, however, more extensive biological experiments will be needed in future to further substantiate our findings.

CONCLUSION

In conclusion, the copper-free, minimalist photo-cross-linkers disclosed in this work have led to successful development of the first affinity-based probes capable of both imaging and covalent labeling of endogenous BRD-4 in live mammalian cells. Key features of cyclopropenes used in these novel linkers, with unique C-1 linkage to protein-targeting moiety, are their tunable reactivity and solubility, relative stability and synthetic accessibility. With an increasing number of terminal alkyne-containing chemical probes available in the literature,[3] some may be converted to their cyclopropene-containing counterparts using the chemistry developed herein for future copper-free, chemical profiling applications. From our study, we have successfully carried out in situ proteome profiling in live HepG2 cells. Subsequent large-scale pull-down/LC−MS/MS experiments have resulted in the identification of several hundred candidate proteins targeted by (+)-JQ1. With the dual capability of our second-generation minimalist probes in simultaneous live-cell imaging and in situ proteome profiling, and the availability of different reporter tags, these unique features were further exploited to narrow down a list of high-confidence off-targets of (+)-JQ1, two of which were subsequently validated by preliminary experiments.

MATERIALS AND METHODS

General Information. All chemicals were purchased from commercial vendors and used without further purification, unless indicated otherwise. All reactions requiring anhydrous conditions were carried out under argon or nitrogen atmosphere using oven-dried glassware. HPLC-grade solvents were used for all reactions. Reaction progress was monitored by TCL on precoated silica plates (Merck 60 $F_{254\ nm}$, 0.25 μm) and spots were visualized by UV, iodine or other suitable stains. Flash column chromatography was carried out using silica gel (Merck 60 $F_{254\ nm}$). All NMR spectra (^{1}H NMR, ^{13}C NMR) were recorded on Bruker 300/500 MHz NMR spectrometers. Chemical shifts are reported in parts per million referenced to appropriate internal standards or residual solvent peaks ($CDCl_3$ = 7.26 ppm, DMSO-d_6 = 2.50 ppm). The following abbreviations were used in reporting spectra, br s (broad singlet), s (singlet), d (doublet), t (triplet), q (quartet), m (multiplet), dd (doublet of doublets). Mass spectra were obtained on Shimadzu IT-TOF-MS or Shimadzu ESI-MS system. All analytical HPLC were carried out on Shimadzu LC−MS (IT-TOF) system or Shimadzu LC−MS-2010EV system equipped with an autosampler using reverse-phase Phenomenex Luna 5 μm $C_{18(2)}$ 100 Å 50 × 3.0 mm columns. Water with 0.1% TFA and acetonitrile with 0.1% TFA were used as eluents and the flow rate was 0.6 mL/min.

HepG2 cells were cultured in Dulbecco's modified Eagle medium (DMEM; Invitrogen) containing 10% heat-inactivated fetal bovine serum (FBS; Invitrogen), 100 units/mL penicillin, and 100 μg/mL streptomycin (Thermo Scientific) and maintained in a humidified 37 °C incubator with 5% CO_2. To generate protein lysates, cells were washed twice with cold phosphate-buffered saline (PBS), harvested with 1× trypsin or by use of a cell scraper, and collected by centrifugation. Cell pellets were then washed with PBS and lysed with 25 mM *N*-(2-hydroxyethyl)piperazine-*N*-2-ethanesulfonic acid (HEPES) buffer (with 150 mM NaCl, and 2 mM $MgCl_2$, *p*H 7.5) containing 0.1% NP-40. Protein concentration was determined by Bradford protein assay. For Western blotting (WB) experiments, samples from HepG2 cells were resolved by SDS−PAGE and transferred to poly(vinylidene difluoride) membranes. Membranes were then blocked with 3% BSA in TBST (0.1% Tween in Tris-buffered saline) for 1 h at room temperature. After blocking, membranes were incubated with the corresponding primary antibody for another hour. After incubation, membranes were washed with TBST (4 × 10 min) and then incubated with an appropriate secondary antibody. Finally, blots were washed again with TBST before being developed with SuperSignal West Dura Kit (Thermo Scientific). BRD-4 recombinant protein was expressed and purified as described

dx.doi.org/10.1021/ja502780z | J. Am. Chem. Soc. 2014, 136, 9990−9998

previously.[24a,27] Antibodies against BRD-4 (ab75898), DDB1 (EPR6089) and RAD23B (ab86781) were purchased from Abcam.

Kinetic studies of tetrazine-cyclopropene ligation were performed mostly based on refs 18−20, with details provided in the Supporting Information.

*Ethyl 2-(2-(3-(2-iodoethyl)-3H-diazirin-3-yl)ethyl)cycloprop-2-enecarboxylate (**L4**).*[9] A 50 mL two-neck round-bottom flask was charged with **L3** (1.48 g, 6.0 mmol, 3.0 equiv), $Rh_2(OAc)_4$ (44 mg, 0.01 mmol, 0.05 equiv) and dichloromethane (DCM; 20 mL). A solution of ethyl diazoacetate (0.23 g, 2.0 mmol, 1 equiv) in DCM (5 mL) was added via a syringe pump in 10 h. The solvent was removed in vacuo, and the residue was purified by flash column chromatography (10:1 hexane:EtOAc) to afford the desired product **L4** as a colorless oil (0.14 g, 21%): ^{1}H NMR (500 MHz, $CDCl_3$) δ 6.46 (s, 1H), 4.13 (m, 2H), 2.82 (t, J = 7.5, 2H), 2.34 (m, 2H), 2.16 (s, 1H), 2.09 (t, J = 7.5, 2H), 1.77 (m, 2H), 1.25 (t, J = 7.2, 3H); ^{13}C NMR (125 MHz, $CDCl_3$) δ 175.94, 113.74, 96.05, 60.38, 37.20, 29.88, 28.35, 19.96, 19.86, 14.38, −4.16; HR-MS (ESI) calcd for $[M + Na]^+$ 357.0076, found 357.0063.

*(2-(2-(3-(2-Iodoethyl)-3H-diazirin-3-yl)ethyl)cycloallyl)methanol (**L7**).* To a stirred solution of **L4** (33.4 mg. 0.1 mmol) in 3 mL of toluene was added 0.5 mL of 1.0 M DIBAL (0.5 mmol, 5 equiv) at −78 °C. The mixture was stirred for 1 h and quenched by addition of 1 N HCl (3 mL). Upon extraction by 2 × 10 mL of EtOAc, the organic phase was concentrated in vacuo and purified by flash column chromatography (1:3 EtOAc:hexane) to afford **L7** as colorless oil (24 mg, 85%): ^{1}H NMR (300 MHz, $CDCl_3$) δ 6.75 (s, 1H), 3.54 (t, J = 7.5, 2H), 2.80 (t, J = 7.5, 2H), 2.31 (t, J = 7.5, 2H), 2.08 (m, 3H), 1.79 (m, 3H); ^{13}C NMR (75 MHz, $CDCl_3$) δ 123.90, 103.66, 68.09, 37.38, 30.02, 28.46, 20.97, 20.69, −4.07. ESI-MS: m/z calcd for 292.0, found 292.2.

*Ethyl 2-(2-(3-(2-azidoethyl)-3H-diazirin-3-yl)ethyl)cycloprop-2-enecarboxylate (**L5**).* To a solution of **L4** (334 mg, 1.0 mmol) in 10 mL of DMF was added sodium azide (78 mg, 1.2 mmol), and the resulting mixture was stirred at room temperature for 12 h and then quenched with 10 mL of water. Upon extraction with EtOAc (2 × 10 mL), the organic layers were washed with saturated aqueous NaCl (10 mL) and dried with anhydrous Na_2SO_4. The solvents were removed in vacuo, and the crude product was purified by flash column chromatography (10:1 hexane:EtOAc) to yield **L5** (214 mg, 86%) as a colorless oil: ^{1}H NMR (300 MHz, $CDCl_3$) δ 6.44 (s, 1H), 4.13 (m, 2H), 3.14 (t, J = 7.5, 2H), 2.34 (t, J = 7.5, 2H), 2.16 (s, 1H), 1.74−1.69 (m, 4H), 1.27 (t, J = 7.5, 3H); ^{13}C NMR (75 MHz, $CDCl_3$) δ 176.41, 113.77, 96.81, 60.17, 46.06, 32.13, 30.22, 26.21, 19.85, 19.78, 14.26.

*Ethyl 2-(2-(3-(2-aminoethyl)-3H-diazirin-3-yl)ethyl)cycloprop-2-enecarboxylate (**L6**).* To a solution of **L5** (348 mg, 1.4 mmol) dissolved in THF/water (10:1, 5 mL) was added triphenylphosphine (0.41 g, 1.6 mmol) at room temperature. The reaction mixture was stirred for 10 h before addition of 1 N HCl (3 mL). Upon extraction with diethyl ether, the aqueous layer was neutralized with 1 N NaOH, and the resulting mixture was further extracted with diethyl ether before being concentrated in vacuo to yield the desired product **L6** (223 mg, 76%): ^{1}H NMR (300 MHz, $CDCl_3$) δ 6.46 (s, 1H), 4.14 (m, 2H), 2.51 (t, J = 7.5, 2H), 2.36 (m, 2H), 1.74 (t, J = 7.2, 2H), 1.62 (t, J = 7.2, 2H), 1.27 (t, J = 7.5, 2H); ^{13}C NMR (75 MHz, $CDCl_3$) δ 176.19, 114.11, 95.53, 60.34, 36.42, 35.45, 32.84, 30.84, 27.27, 19.92, 14.27.

BD-1. Compound **S1** was synthesized by following previously reported procedures.[27] To a stirred solution of **S1** (66.4 mg, 0.2 mmol) in DMF (2 mL) was added HOBt (32 mg, 0.24 mmol), EDCI (46 mg, 0.24 mmol), DIEA (52 mg, 0.4 mmol) and **L6** (49 mg, 0.22 mmol). The mixture was stirred for 12 h and diluted with water. Subsequently, the mixture was extracted with 2 × 10 mL EtOAc. The organic phase was washed with brine. Upon solvent evaporation, the residue was purified by flash column (100:1 to 20:1 DCM:MeOH) to afford **BD-1** as a white solid (69 mg, 65%): ^{1}H NMR (500 MHz, $CDCl_3$) δ 7.70 (m, 1H), 7.51−7.30 (m, 8H), 6.84 (br, 1H), 6.49 (s, 1H), 4.58 (t, J = 7.5 Hz, 1H), 4.13 (m, 2H), 3.54 (m, 1H), 3.36 (m, 1H), 3.13 (m, 2H), 2.66 (s, 3H), 2.30 (m, 2H), 2.13 (s, 1H), 1.69 (m, 2H), 1.64 (m, 2H), 1.28 (t, J = 7.5 Hz, 3H); ^{13}C NMR (125 MHz, $CDCl_3$) δ 176.27, 170.62, 167.74, 138.73, 131.97, 131.54, 130.65, 129.41, 129.30, 128.19, 127.14, 123.12, 111.78, 95.90, 60.34, 53.71, 39.31, 34.81, 32.31, 30.10, 26.65, 19.94, 19.86, 14.26, 12.15; HR-MS (ESI) calcd for $[M + Na]^+$ 560.2386, found 560.2392.

BD-2. To a stirred solution of **BD-1** (10 mg, 0.019 mmol) in 2 mL toluene was added 0.1 mL of 1.0 M DIBAL (in Hexane, 0.1 mmol, 5 equiv) at −78 °C. The mixture was stirred for 2 h and subsequently quenched by addition of 1 N HCl (2 mL). Upon extraction with EtOAc (2 × 10 mL), the combined organic layers were dried over Na_2SO_4 and concentrated in vacuo, and the resulting residue was purified by flash column (50:1 to 20:1 DCM:MeOH), affording the desired product **BD-2** (4 mg, 43%): ^{1}H NMR (500 MHz, $CDCl_3$) δ 7.73 (m, 2H), 7.54 (m, 5H), 7.39 (m, 2H), 7.16 (br, 1H), 6,72 (m, 1H), 4.63 (m, 1H), 3.75 (m, 1H), 3.68 (m, 1H), 3.48 (m, 1H), 3.35 (m, 1H), 3.28 (m, 1H), 3.10 (m, 1H), (d, J = 7.0 Hz, 1H), 2.67 (s, 3H), 2.37 (m, 3H), 1.71 (m, 2H), 1.67 (m, 2H); ^{13}C NMR (125 MHz, $CDCl_3$) δ 173.23, 139.08, 137.54, 133.45, 131.90, 130.24, 128.74, 127.56, 126.18, 124.14, 120.36, 117.80, 112.90, 103.68, 71.71, 67.98, 54.16, 53.40, 39.27, 38.51, 33.91, 32.09, 27.47, 22.86, 21.10, 14.12, 12.34; HR-MS (ESI) calcd for $[M + Na]^+$ 518.2280, found 518.2271.

BD-3. Linker **L2** was obtained by following previously reported procedures.[9] To a stirred solution of compound **S1** (70 mg, 0.22 mmol) in DMF (2 mL) were added HOBt (32 mg, 0.24 mmol), EDCI (46 mg, 0.24 mmol), triethylamine (52 mg, 0.4 mmol) and **L2** (30 mg, 0.22 mmol). The mixture was stirred for 12 h and diluted with water. Subsequently, the mixture was extracted with EtOAc (2 × 10 mL), and the organic phase was washed with brine (2 × 10 mL). Upon solvent evaporation, the resulting residue was purified by flash column (100:1 to 20:1 DCM:MeOH), affording the desired product **BD-3** as a white solid (60 mg, 67%): ^{1}H NMR (500 MHz, $CDCl_3$) δ 7.70 (m, 1H), 7.55−7.29 (m, 8H), 6.84 (br, 1H), 4.64 (t, J = 7.5 Hz, 1H), 3.65 (m, 1H), 3.41 (m, 1H), 3.21 (m, 2H), 2.68 (s, 3H), 2.02 (m, 2H), 1.65 (m, 4H); ^{13}C NMR (125 MHz, $CDCl_3$) δ 170.58, 167.78, 138.72, 133.25, 131.98, 131.55, 130.67, 129.41, 129.29, 128.20, 127.36, 123.34, 82.85, 69.30, 53.71, 39.34, 34.34, 32.60, 31.94, 29.62, 26.67, 13.15, 12.16; HR-MS (ESI) calcd for $[M + Na]^+$ 474.2018, found 474.2018.

Isothermal Titration Calorimetry. Experiments were performed on an ITC200 calorimeter (GE Amersham) interfaced with a computer for data acquisition and analysis using Origin 7 software (Microcal Inc., Northampton, MA). The binding isotherms were best-fit to a one-set binding-site model by Marquardt nonlinear least-squares analysis to obtain binding stoichiometry (N), association constant (K_a), change in enthalpy (ΔH), and change in entropy (ΔS). The free energy (ΔG) and ΔS were calculated by the following equations, respectively: $\Delta G = -RT \ln K_a$; $\Delta S = (\Delta H - \Delta G)/T$. Recombinantly purified $(His)_6$-tagged BRD-4 protein[27] was extensively dialyzed against 20 mM HEPES buffer (with 150 mM NaCl, pH 7.4), and the same buffer was used for reconstituting small molecule ligands. The experiments were carried out by titration of 20 μM of the protein in the sample cell with 400 μM of a ligand in the titration syringe. The cell was thermostated at 25 °C, and uniform mixing was ensured by continuous stirring of titration syringe at 400 rpm. All titration experiments were performed by addition of 2 μL titrant per injection, with 20 injections spaced at 200-s intervals.

In Vitro and In Situ Protein Labeling. For gel-based protein/cell lysate labeling experiments, procedures were based mostly on previously published protocols with some modifications.[9] For labeling of recombinant BRD-4, to 2 μg of the protein in 50 μL of PBS buffer was added different concentrations of the probe, and the reaction was incubated for 30 min at room temperature with gentle shaking. Subsequently, the reactions were UV-irradiated (350 nm) for 20 min followed by conjugating with a suitable "click" reporter. For probes **BD-3** and **NP-1**, rhodamine azide **TER-N$_3$** (in 50 μM final concentration from 1 mM DMSO stock[9]) under catalysis of $CuSO_4$ (1 mM final concentration from 100 mM freshly prepared stock solution in deionized water), TBTA (100 μM final concentration from 10 mM freshly prepared stock solution in DMSO) and TCEP (1 mM final concentration from 100 mM freshly prepared stock solution in deionized water) were used. For **BD-1**, **-2** and **NP-2**, **TER-TZ1** (50

μM final concentration from 1 mM freshly prepared DMSO stock) was used with ligation time of 2 h (for concentration-dependent labeling experiments), or 1−60 min (for time-dependent labeling). For bacterial lysate labeling, 1 μM of the probe and 2 μg of the lysate were used, together with 10 μM of **TER-TZ1** (with 2 h tetrazine-cyclopropene ligation time). Subsequently, 10 μL of 6× SDS loading dye was added, and the mixture was heated at 95 °C for 10 min. The resulting proteins were separated by SDS-PAGE. In-gel fluorescence scanning (FL) was used to visualize the labeled protein bands. Coomassie staining (CBB) was used to detect the total amount of loaded proteins.

For in situ proteome labeling and PD/WB experiments (e.g., Figure 3E,G), either 1 or 5 μM of each probe, with or without 10(+)-JQ1 as the competitor, was used. Briefly, after cells were grown, the medium was removed, and cells were washed twice with cold PBS and then treated with 0.5 mL of the DMEM-containing probe (diluted from DMSO stocks whereby DMSO never exceeded 1% in the final solution). After 2−4 h of incubation at 37 °C/5% CO_2, the medium was aspirated, and cells were washed gently with 2× PBS to remove excessive probe, followed by UV irradiation for 20 min on ice. The cells were trypsinized and pelleted by centrifugation. Eventually, the cell pellets were resuspended in HEPES buffer (50 μL), homogenized by sonication, and diluted to 1 mg/mL with PBS. To 50 μL of the resulting proteome solution was added **TER-TZ1** (50 μM final concentration from 1 mM freshly prepared DMSO stock). The reaction was further incubated for 2 h with gentle mixing, before being terminated by addition of prechilled acetone (0.5 mL; 30 min incubation at −20 °C). Precipitated proteins were subsequently collected by centrifugation (13 000 rpm × 10 min at 4 °C). The supernatant was discarded, and the pellet was washed with 200 μL of prechilled methanol, 2 × loading buffer was added and heated for 10 min at 95 °C. Around 20 μg (per gel lane) of proteins were separated by SDS−PAGE and visualized by in-gel fluorescence scanning. Subsequently, the remaining portion of the probe-labeled proteome (prior to tetrazine ligation reaction) was added **Biotin-TZ2** (50 μM final concentration from 1 mM freshly prepared DMSO stock). The mixture was incubated at room temperature for 2 h with gentle mixing, acetone precipitated, and resolubilized in 1% SDS (in PBS) with brief sonication. This resuspended sample was then incubated with avidin-agarose beads (100 μL/mg protein) overnight at 4 °C. Upon centrifugation, the supernatant was removed, and the beads were washed with 0.1% SDS once and PBS (4×), then boiled in 1 × SDS loading buffer for 15 min. Control PD using the negative probe (**NP-2**), and the reference probe (**BD-3**) were carried out concurrently.

Live-Cell Imaging. The experiments were mostly based on previously published protocols.[9,12a,c] HepG2 cells seeded in glass bottom dishes (Mattek) and grown until 70−80% confluency were treated with 0.3 mL of DMEM with a probe or **NP-2** at different indicated concentrations, with or without 10(+)-JQ1. After incubation for 2 h, the medium was removed and cells were gently washed twice with PBS, followed by UV irradiation (350 nm) for 20 min on ice. Cells were then incubated in DMEM containing **FL-TZ1** (50 μM final concentration) for 1−60 min at 37 °C, and washed with fresh DMEM medium (10 min to 2 h) before being imaged. We also tried the no-wash, direct imaging protocol,[12a] but it resulted in higher fluorescence background. Images shown in Figure 3D were results obtained from 2 h DMEM wash. In the last 20 min of incubation, Hochest nuclear stain (1:30 000 dilution) was added to the incubation medium. For immunofluorescence (IF) experiments, after live-cell imaging, the cells were fixed for 1 h at room temperature with 3.7% formaldehyde in PBS, washed twice with cold PBS again, and permeabilized with 0.1% Triton X-100 in PBS for 10 min. Cells were then blocked with 2% BSA in PBS for 30 min, washed twice with PBS, and further incubated with *anti*-BRD-4 antibody (1:100 dilution) for 1 h at room temperature, washed twice with PBS, and then incubated with Cy3-labeled goat antirabbit (Invitrogen 81−6115, 1:100 dilution) for 1 h, following by washing again with PBS before imaging. All imaging data were collected on a Leica TCS SP5X confocal microscope system and images were processed as previously described.[12c]

Large-Scale Protein Identification by LC−MS/MS. Pull-down experiments were carried out as above-described, separated on 10% SDS-PAGE gels, followed by Coomassie staining and tryptic digestion as previously described.[9] Digested peptides were extracted from the gel, separated on a Shimadzu UFLC system (Shimadzu, Japan) coupled to an Orbitrap Elite (Thermo Electron, Germany). The Orbitrap Elite was set to perform data acquisition in the positive-ion mode, except that the m/z range of 350−1600 was used in the full MS scan. The raw data were converted to mgf format. The database search was performed with an in-house Mascot server (version 2.2.07, Matrix Science) with MS tolerance of 10 ppm and MS/MS tolerance of 0.8 Da. Two missed cleavage sites of trypsin were allowed. Carbamidomethylation (C) was set as a fixed modification, and oxidation (M) and phosphorylation (S, T, and Y) were set as variable modifications. All LC−MS/MS samples were injected at least twice, and proteins that appeared in duplicated/triplicated runs (~75% on average) were further processed. Results obtained from the above experiments (in situ, and negative probe) were processed as shown below, and complete MS results are summarized in the Supporting Information. Finally, we ranked the protein hits by their protein scores and emPAI values. The Exponentially Modified Protein Abundance Index (emPAI) offers approximate, label-free, relative quantitation of proteins in a mixture based on protein coverage by the peptide matches in a database search result.[28] Selected MS results are summarized in Tables 1, S2 and S3 (Supporting Information). "False" hits that appeared in negative control PD/LC−MS/MS experiments were eliminated. For runs obtained with 10(+)-JQ1, proteins were deemed potential hits if their protein scores were significantly lowered (or did not appear) in the presence of the competitor. Subcellular localizations of potential hits were determined by checking individual proteins against www.genecards.org.

Preliminary Target Validation. The pull-down samples were prepared as above-described, separated by 10% SDS gel and transferred to poly(vinylidene difluoride) membranes. The WB procedures were carried out as above-described, with the respective antibodies (1:5000 and 1:2000 dilutions for DDB1 and RAD23B, respectively).

■ ASSOCIATED CONTENT

Supporting Information

Other relevant experimental sections, characterization of new compounds, supplementary chemical, biological and LC−MS/MS results. This material is available free of charge via the Internet at http://pubs.acs.org.

■ AUTHOR INFORMATION

Corresponding Author

chmyaosq@nus.edu.sg

Notes

The authors declare no competing financial interest.

■ ACKNOWLEDGMENTS

Funding was provided by the National Medical Research Council (CBRG/0038/2013) and Ministry of Education (MOE2012-T2-1-116/MOE2012-T2-2-051). We acknowledged contributions from Dr. Chongjing Zhang for his initial work, and Ramya Chandrasekaran for expression of recombinant BRD-4 protein.

■ REFERENCES

(1) Ziegler, S.; Pries, V.; Hedberg, C.; Waldmann, H. *Angew. Chem., Int. Ed.* **2013**, *52*, 2744−2792.

(2) Simon, G. M.; Niphakis, M. J.; Cravatt, B. F. *Nat. Chem. Biol.* **2013**, *9*, 200−205.

(3) Su, Y.; Ge, J.; Zhu, B.; Zheng, Y.-G.; Zhu, Q.; Yao, S. Q. *Curr. Opin. Chem. Biol.* **2013**, *17*, 768−775.

(4) Cravatt, B. F.; Wright, A. T.; Kozarich, J. W. *Annu. Rev. Biochem.* **2008**, *77*, 383−414.
(5) Lee, J.; Bogyo, M. *Curr. Opin. Chem. Biol.* **2013**, *17*, 118−126.
(6) Park, J.; Koh, M.; Park, S. B. *Mol. BioSyst.* **2013**, *9*, 544−550.
(7) Yang, P. -Y; Liu, K.; Ngai, M. H.; Lear, M. J.; Wenk, M. R.; Yao, S. Q. *J. Am. Chem. Soc.* **2010**, *132*, 656−666.
(8) Shi, H.; Zhang, C.-J.; Chen, G. Y. J.; Yao, S. Q. *J. Am. Chem. Soc.* **2012**, *134*, 3001−3014.
(9) Li, Z.; Hao, P.; Li, L.; Tan, C.Y. J.; Cheng, X.; Chen, G. Y. J.; Sze, S. K.; Shen, H.-M.; Yao, S. Q. *Angew. Chem., Int. Ed.* **2013**, *52*, 8551−8556.
(10) Kolb, H. C.; Sharpless, K. B. *Drug Discovery Today* **2003**, *8*, 1128−1137.
(11) For a recent review, see Dubinsky, L.; Krom, B. P.; Meijler, M. M. *Bioorg. Med. Chem.* **2012**, *20*, 554−570 and references cited therein.
(12) (a) Yang, K. S.; Budin, G.; Reiner, T.; Vinegoni, C.; Weissleder, R. *Angew. Chem., Int. Ed.* **2012**, *51*, 6598−6603. (b) Budin, G.; Yang, K. S.; Reiner, T.; Weissleder, R. *Angew. Chem., Int. Ed.* **2011**, *50*, 9378−9381. (c) Li, L.; Shen, X.; Xu, Q.-H.; Yao, S. Q. *Angew. Chem., Int. Ed.* **2013**, *52*, 424−428. (d) Li, L.; Ge, J.; Wu, H.; Xu, Q.- H.; Yao, S. Q. *J. Am. Chem. Soc.* **2012**, *134*, 12157−12167. (e) Hu, M.; Li, L.; Wu, H.; Su, Y.; Yang, P.-Y.; Uttamchandani, M.; Xu, Q.-H.; Yao, S. Q. *J. Am. Chem. Soc.* **2011**, *133*, 12009−12020. (f) Edgington, L. E.; Berger, A. B.; Blum, G.; Albrow, V. E.; Paulick, M. G.; Lineberry, N.; Bogyo, M. *Nat. Med.* **2009**, *15*, 967−973. (g) Pratt, M. R.; Sekedat, M. D.; Chiang, K. P.; Muir, T. W. *Chem. Biol.* **2009**, *16*, 1001−1012. (h) Watzke, A.; Kosec, G.; Kindermann, M.; Jeske, V.; Nestler, H. P.; Turk, V.; Turk, B.; Wendt, K. U. *Angew. Chem., Int. Ed.* **2008**, *47*, 406−409.
(13) Yang, K. S.; Budin, G.; Tassa, C.; Kister, O.; Weissleder, R. *Angew. Chem., Int. Ed.* **2013**, *52*, 10593−10597.
(14) (a) Kwan, D. H.; Chen, H.-M.; Ratananikom, K.; Hancock, S. M.; Watanabe, Y.; Kongsaeree, P. T.; Samuels, A. L.; Withers, S. G. *Angew. Chem., Int. Ed.* **2011**, *50*, 300−303. (b) Ge, J.; Li, L.; Yao, S. Q. *Chem. Commun.* **2011**, *47*, 10939−10941.
(15) Sletten, E. M.; Bertozzi, C. R. *Angew. Chem., Int. Ed.* **2009**, *48*, 6974−6998.
(16) Devaraj, N. K.; Weissleder, R. *Acc. Chem. Res.* **2011**, *44*, 816−827.
(17) Selvaraj, R.; Fox, J. M. *Curr. Opin. Chem. Biol.* **2013**, *17*, 753−760.
(18) Yang, J.; Šečkutė, J.; Cole, C. M.; Devaraj, N. K. *Angew. Chem., Int. Ed.* **2012**, *51*, 7476−7479.
(19) Patterson, D. M.; Nazarova, L. A.; Xie, B.; Kamber, D. N.; Presche, J. A. *J. Am. Chem. Soc.* **2012**, *134*, 18638−18643.
(20) Kamber, D. N.; Nazarova, L. A.; Liang, Y.; Lopez, S. A.; Patterson, D. M.; Shih, H.-W.; Houk, K. N.; Prescher, J. A. *J. Am. Chem. Soc.* **2013**, *37*, 13680−13683.
(21) Yu, Z.; Pan, Y.; Wang, Z.; Wang, J.; Lin, Q. *Angew. Chem., Int. Ed.* **2012**, *51*, 10600−10604.
(22) Yan, N.; Liu, X.; Pallerla, M.; Fox, J. M. *J. Org. Chem.* **2008**, *73*, 4283−4286.
(23) Berger, S. L. *Nature* **2007**, *447*, 407−412.
(24) (a) Filippakopoulos, P.; Qi, J.; Picaud, S.; Shen, Y.; Smith, W. B.; Fedorov, O.; Morse, E. M.; Keates, T.; Kickman, T. T.; Felletar, I.; Philpott, M.; Munro, S.; McKeown, M. R.; Wang, Y.; Christie, A. L.; West, N.; Cameron, M. J.; Schwartz, B.; Heightman, T. D.; Thangue, N. L.; French, C. A.; Wiest, O.; Kung, A. L.; Knapp, S.; Brandner, J. E. *Nature* **2010**, *468*, 1067−1073. (b) Nicodeme, E.; Jeffrey, K. L.; Schaefer, U.; Beinke, S.; Dewell, S.; Chung, C.-W.; Chandwani, R.; Marazzi, I.; Wilson, P.; Coste, H.; White, J.; Kirilovsky, J.; Rice, C. M.; Lora, J. M.; Prinjha, R. K.; Lee, K.; Tarakhovsky, A. *Nature* **2010**, *468*, 1119−1123.
(25) (a) Delmore, J. E.; Issa, G. C.; Lemieux, M. E.; Peter B. Rahl, P. B.; Shi, J.; Jacobs, H. M.; Kastritis, E.; Gilpatrick, T.; Paranal, R. M.; Qi, J.; Chesi, M.; Schinzel, A. C.; McKeown, M. R.; Heffernan, T. P.; Vakoc, C. R.; Bergsagel, P. L.; Ghobrial, I. M.; Richardson, P. G.; Young, R. A.; Hahn, W. C.; Anderson, K. C.; Kung, A. L.; Bradner, J. E.; Mitsiades, C. S. *Cell* **2011**, *146*, 904−917. (b) Floyd, S. R.; Pacold, M. E.; Huang, Q.; Clarke, S. M.; Lam, F. C.; Cannell, I. G.; Bryson, B. D.; Rameseder, J. R.; Lee, M. J.; Blake, E. J.; Fydrych, A.; Ho, R.; Greenberger, B. A.; Chen, G. C.; Maffa, A.; Del Rosario, A. M.; Root, D. E.; Carpenter, A. E.; Hahn, W. C.; Sabatini, D. M.; Chen, C. C.; White, F. M.; Bradner, J. E.; Yaffe, M. B. *Nature* **2013**, *498*, 246−250.
(26) Chung, C.-W.; Coste, H.; White, J. H.; Mirguet, O.; Wilde, J.; Gosmini, R. L.; Delves, C.; Magny, S. M.; Woodward, R.; Hughes, S. A.; Boursier, E. V.; Flynn, H.; Bouillot, A. M.; Bamborough, P.; Brusq, J. -M. G.; Gellibert, F. J.; Jones, E. J.; Riou, A. M.; Homes, P.; Martin, S. L.; Uings, I. J.; Toum, J.; Clement, C. A.; Boullay, A.-B.; Grimley, R. L.; Blandel, F. M.; Prinjha, R. K.; Lee, K.; Kirilovsky, J.; Nicodeme, E. *J. Med. Chem.* **2011**, *54*, 3827−3838.
(27) Zhang, C.; Tan, C. Y. J.; Na, Z.; Ge, J.; Chen, G. Y. J.; Uttamchandani, M.; Sun, H.; Yao, S. Q. *Angew. Chem., Int. Ed.* **2013**, *52*, 14060−14064.
(28) (a) Ishihama, Y.; Oda, Y.; Tabata, T.; Sato, T.; Nagasu, T.; Rappsilber, J.; Mann, M. *Mol. Cell. Proteomics* **2005**, *4*, 1265−1272. (b) Hao, P.; Guo, T.; Li, X.; Adav, S. S.; Yang, J.; Wei, M.; Sze, S. K. *J. Proteome Res.* **2010**, *9*, 3520−352.